Dynamics of mobile ions in single- and mixed-cation glasses

Dynamics of mobile ions in single- and mixed-cation glasses

C Cramer[1], S Brunklaus, Y Gao and K Funke

Westfälische Wilhelms-Universität, Institut für Physikalische Chemie and
Sonderforschungsbereich 458, Schlossplatz 4/7, 48149 Münster, Germany

E-mail: CramerC@uni-muenster.de

Abstract
To study the ion dynamics of several inorganic glasses, including single-
and mixed-cation glasses, we have determined conductivity spectra over wide
ranges in frequency. In the case of the single-cation glasses, these spectra extend
from a few hertz up to the terahertz regime. The spectra show a transition
from their dc values to a dispersive regime where the conductivity increases
continuously with frequency, tending towards a linear frequency dependence
at sufficiently low temperatures. At high frequencies the dynamic conductivity
is governed by vibrational contributions, whereas ionic hopping sequences
determine the low-frequency part of the spectra. In an intermediate-frequency
regime, both hopping and vibrational contributions contribute to the dynamic
conductivity. The shape of the high-frequency conductivity spectra is discussed
for various glasses. The low-frequency spectra are discussed in the framework
of the concept of mismatch and relaxation.

For the mixed-cation glasses where spectra have been taken by impedance
spectroscopy, we report on a new kind of mixed-alkali effect. In contrast to
conductivity spectra of single-cation glasses which follow the time–temperature
superposition principle, featuring a temperature-invariant shape, the shapes of
the conductivity spectra of the mixed-alkali glasses studied here are found to
change with temperature. To explain this effect, we suggest differently activated
mobilities of the two different ionic species.

1. Introduction

The dynamics of mobile ions in ion-conducting glasses constitute one of the major unsolved
problems in the field of solid-state ionics. In contrast to structurally disordered crystalline
electrolytes, glassy materials do not provide easy access to their structural properties.

---

[1] Author to whom any correspondence should be addressed.

Therefore, little is known even about possible sites for the mobile ions within the glassy network. This lack of structural knowledge substantially complicates the study of the elementary steps of ion transport.

In the last few years, endeavors to obtain a better understanding of the ion dynamics in glass have been made along two different lines of experimental investigation. One of them is concerned with the identification of ionic sites on the basis of infrared and Raman spectra [1–4], or by nuclear magnetic resonance techniques [5, 6]. The other relies on extracting information about the hopping dynamics from frequency-dependent conductivities which are normally measured by impedance spectroscopy [7, 8]. However, one of the major drawbacks of impedance spectroscopy is its limitation to frequencies below the megahertz regime. As a consequence, this technique provides a view on the ion dynamics at comparatively long times only, without reflecting the development of correlations in the movements of ions that occur on shorter timescales. In order to bridge the gap between the traditional impedance frequency regime and the far infrared, and thus to probe the short-time hopping dynamics, we have performed additional measurements of the ionic conductivity at radio, microwave, millimetre and sub-millimetre wave frequencies. In the following, we will first discuss the conductivity spectra of one lithium-ion-conducting glass, namely $B_2O_3 \cdot 0.56Li_2O \cdot 0.45LiBr$, and of two silver-ion-conducting glasses, $0.5AgI \cdot 0.5AgPO_3$ and $0.48(AgI)_2 \cdot 0.52Ag_2SeO_4$. These conductivity spectra extend from infrared frequencies down to a few hertz and thus probe the transition from elementary steps to macroscopic transport. The latter part of this paper discusses mixed-cation glasses with mobile alkali ions of two kinds where spectra have been taken by impedance spectroscopy. Here, we report on a new kind of mixed-alkali effect occurring in the shapes of the conductivity spectra which are found to change with temperature.

2. Single-cation glasses: results

Figure 1 shows conductivity isotherms of glassy $B_2O_3 \cdot 0.56Li_2O \cdot 0.45LiBr$ in a log–log representation of $\sigma(\nu)T$ versus the experimental frequency ν at four temperatures T. The results presented here confirm the following basic facts that are well known from impedance spectroscopy.

(1) The temperature dependence of the dc conductivity, σ_{dc}, is well described by the Arrhenius law, reflecting the activated nature of ionic hopping processes.
(2) Ion-conducting glasses display an increase of their ionic conductivity as a function of frequency. At sufficiently low frequencies ν, $\sigma(\nu)$ *roughly* follows the Jonscher power law [9],

$$\sigma(\nu) \approx \sigma_{dc}(1 + (\nu/\nu_0)^p). \tag{1}$$

Here, ν_0 marks the onset of the conductivity dispersion on the frequency scale. Reported values of the exponent p typically range from 0.5 to 0.7.
(3) With increasing normalized conductivity, $\sigma(\nu)/\sigma_{dc}$, equation (1) becomes more and more inappropriate. In fact, the apparent exponent is found to vary with the ratio $\sigma(\nu)/\sigma_{dc}$, increasing gradually and tending towards unity for large values of $\sigma(\nu)/\sigma_{dc}$, then corresponding to a nearly frequency-independent dielectric loss [10, 11].
(4) Glassy electrolytes are usually found to obey the so-called time–temperature superposition principle [12–14]. This means that their low-frequency ionic conductivities collapse onto a single 'master curve', if the conductivity and the frequency axes are scaled in an appropriate way, e.g. if $\log(\sigma(\nu)/\sigma_{dc})$ is plotted versus $\log(\nu/(\sigma_{dc}T))$. This is illustrated in figure 2 for impedance spectra of glassy $B_2O_3 \cdot 0.56Li_2O \cdot 0.45LiBr$ which we have measured recently;
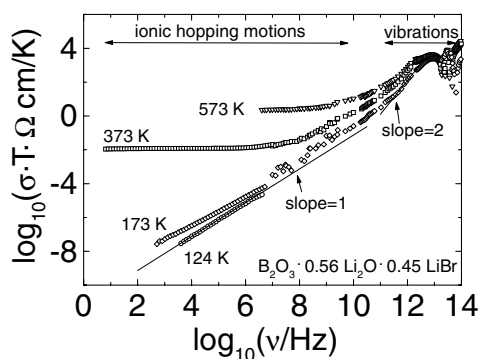
Figure 1. Complete experimental conductivity spectra of glassy $B_2O_3 \cdot 0.56Li_2O \cdot 0.45LiBr$ at various temperatures.

see also [15]. It should be noted that the 148 K isotherm still shows the transition into the dc plateau, the conductivity, therefore, still being caused by activated hopping processes. Figure 2(b) shows the master curve constructed from the data of figure 2(a) by means of the Summerfield scaling procedure [16, 17]. For reasons of clarity only three isotherms are included in the scaled representation, although all other isotherms also fall on the master curve. The scaling procedure applied in figure 2 was first reported for amorphous semiconductors by Summerfield *et al* [16, 17], but seems to be valid also for many ion-conducting glasses [12, 18, 19]. The validity of the Summerfield scaling formalism implies that macroscopic diffusion, which is proportional to $\sigma_{dc}T$ because of the Nernst–Einstein relation, increases with temperature at the same rate as the characteristic frequency ν_0 does. As the shape of the dispersion does not vary with temperature, we may conclude that the mechanism of the underlying ion dynamics is preserved.

While it is clear that the increase of the ionic conductivity with frequency reflects the frequent occurrence of correlated back-and-forth hopping processes of the mobile ions in the glass, the master curve signature of their hopping dynamics does not determine the experimental conductivity spectra at higher frequencies, say, in the microwave regime. In [20] we have discussed in detail such high-frequency spectra for glassy $0.5Ag_2S \cdot 0.5GeS_2$, where the complete experimental spectra could be well described by a superposition of two distinct contributions. The first one is the low-frequency part where the Summerfield scaling is valid, the conductivity being due to ionic hopping processes. The second contribution is a vibrational component where the low-frequency flank of the broad peak shows a ν^2-dependence on frequency at all temperatures.

Turning back to the complete conductivity spectra of glassy $B_2O_3 \cdot 0.56Li_2O \cdot 0.45LiBr$ presented in figure 1, we also see that at frequencies higher than roughly 0.5 THz, all conductivity spectra show a broad peak with a small temperature dependence and a ν^2-dependence on frequency on the low-frequency flank. Such features clearly indicate their vibrational origin and have also been reported for other amorphous materials [21, 22]. In the following, we will focus on frequencies located between the 'low-frequency regime' probing ionic hopping motion and the high-frequency vibrational regime. In order to investigate whether or not the data in the gigahertz regime still follow the time–temperature superposition principle valid at lower frequencies, we compare the shape of the master curve displayed in figure 2 with the shape of the total experimental spectra. Figure 3 shows such a comparison between the experimental data (circles) and the master curve (black line). Note that the master
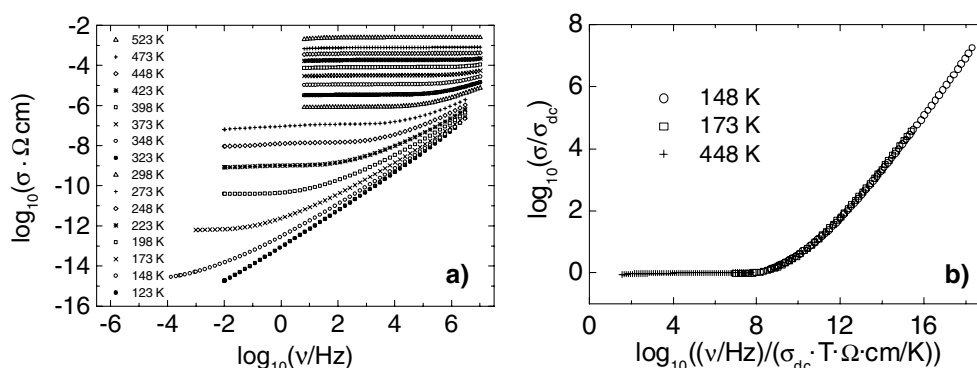
Figure 2. Conductivity spectra of glassy $B_2O_3 \cdot 0.56Li_2O \cdot 0.45LiBr$: (a) experimental spectra at various temperatures; (b) the master curve representation.

curve is rescaled into the $\log(\sigma(\nu))$ versus $\log(\nu)$ representation for reasons of clarity. We directly see from figure 3 that above approximately 1 GHz the experimental data deviate from the master curve. Even below the frequency regime where the vibrational component with a ν^2-dependence on frequency determines the conductivity, the experimental spectrum is steeper than the master curve. We can now subtract at each frequency the master curve contribution from the total spectra. The resulting 'reduced spectrum' (represented by crosses) is shown in figure 3, the frequency regime between $\log(\nu/\text{Hz}) = 9.5$ and 13.5 being highlighted in the inset. The reduced spectrum at 223 K as well as reduced spectra determined at other temperatures, show the following features:

- On the low-frequency flank of the broad vibrational peak we see a ν^2-dependence on frequency at frequencies between 0.5 and 3 THz. However, we also observe a crossover into a $\nu^{1.3}$-dependence on frequency at frequencies below 0.5 THz. This is in contrast to the behaviour reported for glassy $0.5Ag_2S \cdot 0.5GeS_2$ where we observe no change of the ν^2-dependence on frequency into another one [20].
- In the gigahertz regime, the reduced spectra appear to be the extensions of the FIR data (between 0.17 and 0.5 THz) and feature the same $\nu^{1.3}$-dependence on frequency.
- In the entire frequency range between 1 GHz and 3 THz, the temperature dependence of the reduced spectra is very small and does not differ when the frequency dependence changes from $\nu^{1.3}$ to ν^2. Therefore, we think that this complete spectral part is likely to be caused by vibrational-like motion.

We now turn to two other single-cation glasses, namely $0.48(AgI)_2 \cdot 0.52Ag_2SeO_4$ and $0.5AgI \cdot 0.5AgPO_3$, where we have analysed complete conductivity spectra following the same procedure as described above. Complete conductivity spectra of glassy $0.48(AgI)_2 \cdot 0.52Ag_2SeO_4$ have been published earlier; see also [20, 23]. Reduced spectra of this glass are compared with new results on $0.5AgI \cdot 0.5AgPO_3$ glasses. For glassy $0.48(AgI)_2 \cdot 0.52Ag_2SeO_4$, of which one isotherm is shown in figure 4(a), we find that between 10 and 110 GHz the reduced 296 K spectrum coincides with a straight line extrapolated from the far-infrared conductivities. Taking into account other isotherms we obtain the following results:

- At all temperatures, the gigahertz regime of the reduced spectra can be regarded as the extension of the low-frequency flank of the vibrational part as probed at FIR frequencies (between 0.3 and 1 THz).
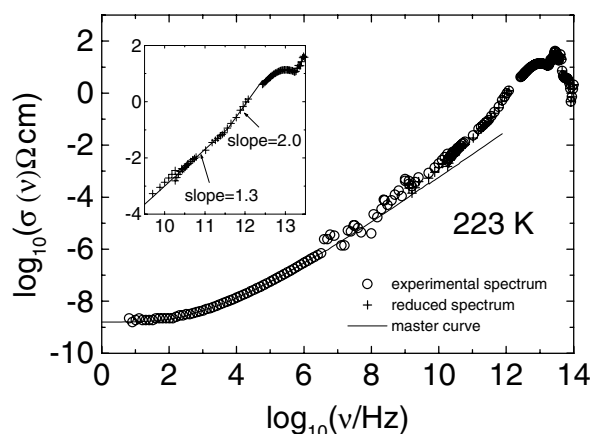
Figure 3. The experimental conductivity spectrum of glassy $B_2O_3 \cdot 0.56Li_2O \cdot 0.45LiBr$ at 223 K (circles) in comparison with the master curve (solid curve) as shown in figure 2(b). The reduced spectra (crosses) result from subtracting the master curve contribution out of the experimental spectrum.
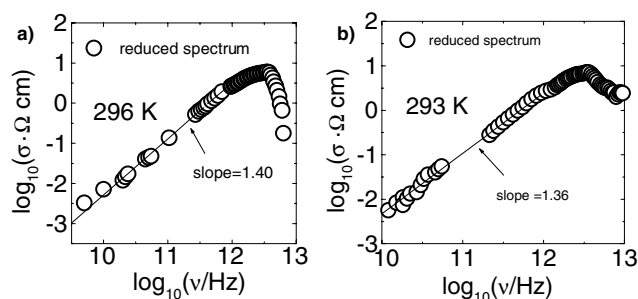

Figure 4. Reduced conductivity spectra of (a) glassy $0.48(AgI)_2 \cdot 0.52Ag_2SeO_4$ and (b) glassy $0.5AgI \cdot 0.5AgPO_3$.

- The frequency dependence on the low-frequency flank is described by ν^q. The value of q is found to increase with decreasing temperature approaching two at our lowest temperatures, namely 93 and 113 K.

The reduced spectra of the third glass, $0.5AgI \cdot 0.5AgPO_3$, one of them being presented in figure 4(b), strongly resemble those of glassy $0.48(AgI)_2 \cdot 0.52Ag_2SeO_4$. Again we find that the low-frequency flank of the vibrational part is well described by ν^q. Like for the selenate glass, the value of q increases with decreasing temperature. The temperature dependence is, however, slightly smaller for the phosphate glass. This can be seen in figure 5 which shows the exponents governing the conductivity spectra in the gigahertz and terahertz regimes at different temperatures for both silver-ion-conducting glasses discussed above.

3. Single-cation glasses: discussion of the results

First we can state that the three different glasses discussed above show the same kind of low-frequency behaviour. Below the gigahertz regime the data follow the time–temperature
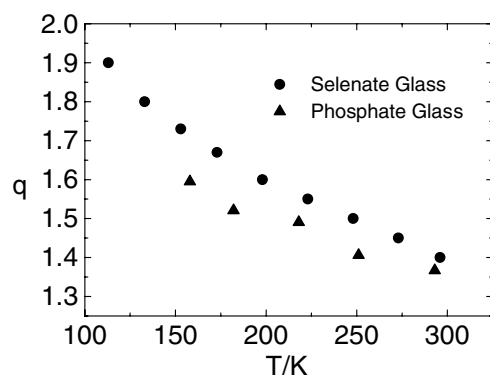
Figure 5. Exponents q governing the frequency dependences in the high-frequency spectra of glassy $0.48(AgI)_2 \cdot 0.52Ag_2SeO_4$ and $0.5AgI \cdot 0.5AgPO_3$.

superposition principle and can be scaled onto a master curve. In the high-frequency regime, the spectra of all single-cation glasses exhibit frequency dependences on the low-frequency flanks of the vibrational peaks which are weaker than ν^2. Whereas a 'classical' ν^2-dependence on frequency in the vibrational regime can be interpreted by rattling motions of ions in harmonic potential landscapes, conductivity components with a weaker frequency dependence might be caused by anharmonic vibrations. According to Jain and co-workers [24], a ν^q-dependence on frequency can also be caused by jellyfish-type local fluctuations of the glass network and the ions included therein.

The differences in the reduced spectra between the various glasses are linked to their structures. Whereas the $B_2O_3 \cdot 0.56Li_2O \cdot 0.45LiBr$ glass is a so-called network glass with a condensed network of BO_3 and BO_4 units, the $0.48(AgI)_2 \cdot 0.52Ag_2SeO_4$ glass only consists of discrete selenate, iodide and silver ions which can move apart from each other easily when the temperature is enhanced. This is most probably why the shape of the vibrational peak changes with temperature in the latter glass, whereas the respective shape does not change with temperature in the network glass. For the $0.5AgI \cdot 0.5AgPO_3$ glass, where the network consists of chains of condensed PO_4 tetrahedra possessing an intermediate degree of connectivity, a temperature dependence on the low-frequency flank of the vibrational part does exist, but it is less pronounced than in the selenate glass. Temperature-dependent shapes of the vibrational spectra as reported for glassy $0.48(AgI)_2 \cdot 0.52Ag_2SeO_4$ and $0.5AgI \cdot 0.5AgPO_3$ are typical of supercooled glass-forming liquids such as CKN which also lack a condensed network [25]. We strongly feel that there is need for additional theoretical work in order to understand the origin of the microscopic dynamics occurring on a picosecond timescale, resulting in 'non-classical' vibrational spectra. MD simulations on alkali borate glasses are currently being performed [26].

In the following, we consider the low-frequency parts of the conductivity spectra and discuss the origin of their master curve signature. As outlined above, conductivity spectra of ion-conducting glasses show a transition from a dc plateau into a dispersive regime where $\partial \log(\sigma(\nu))/\partial \log(\nu)$ increases with frequency. Models such as Ngai's coupling concept [27, 28] and the jump relaxation model [29, 30] have often been used to explain such conductivity spectra. However, they cannot reproduce the experimentally validated transition from a Jonscher-type power-law behaviour to a nearly constant-loss behaviour. The latter transition is, however, well reproduced within the concept of mismatch and relaxation (CMR) which differs from the jump relaxation model by inclusion of a second rate equation. A more
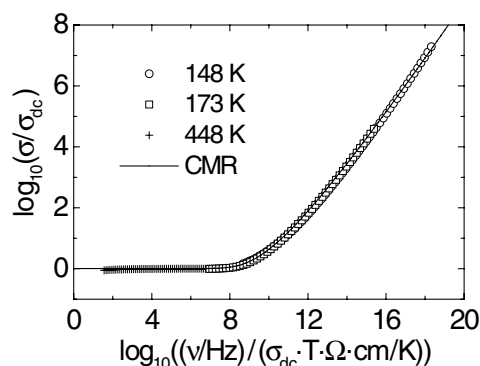
Figure 6. Comparison between the experimental master curve of glassy $B_2O_3 \cdot 0.56Li_2O \cdot 0.45LiBr$ and the master curve obtained from the CMR.

detailed description of the CMR can be found in [12, 31–35]. Here, we only outline the basic assumptions of the model and compare model spectra with the experimental ones.

The central idea of the CMR is the following. Mismatch is created by each hop of a mobile ion. The system then tends to reduce the mismatch, which can be done by a backward hop of the ion itself ('single-particle route') or by rearrangement of its neighbourhood ('many-particle route'). The first rate equation claims that the rates of relaxation along the two routes are always proportional to each other. The second rate equation exploits the fact that the mobile neighbours are of the same kind as the 'central' ion. The rate of relaxation on the 'many-particle route' is thus again related to single-particle functions such as the velocity autocorrelation function. The latter are then obtainable from the two equations in a self-consistent fashion. Local mismatch is, however, not only *reduced* by the rearrangement of the neighbourhood, but at the same time also progressively *shielded*. An empirical parameter K is introduced to quantify the time dependence of the shielding effect. More details are given in [32–35]. The parameter K turns out to modify the shape of the conductivity spectra, increasing values of K resulting in a more gradual onset of the dispersion. This will be discussed in more detail in context with the spectra of the mixed-alkali glasses. For most single-cation glasses and also in many crystals, the value of K is found to be close to 2.0. Such an example is given in figure 6 where the experimental conductivity master curve of glassy $B_2O_3 \cdot 0.56Li_2O \cdot 0.45LiBr$ (shown earlier in figure 2) is compared to the corresponding CMR master curve. The two master curves are found to be in excellent agreement. The validity of the experimentally established time–temperature superposition principle is easily understood in terms of the CMR: temperature changes affect the ion dynamics only by changing the rates of the hopping processes, while the mechanism and the number of ions involved remain unchanged.

4. Mixed-cation glasses: results

In the previous paragraphs we have shown that the low-frequency spectra of three single-cation glasses follow the time–temperature superposition principle and can, therefore, be scaled onto a master curve. While there are only few exceptions from the validity of the time–temperature superposition principle in single-cation glasses [36], we have recently found that the spectra of mixed-alkali glasses cannot be scaled onto a master curve [15]. These deviations from the validity of the time–temperature superposition principle are discussed in more detail in this section.
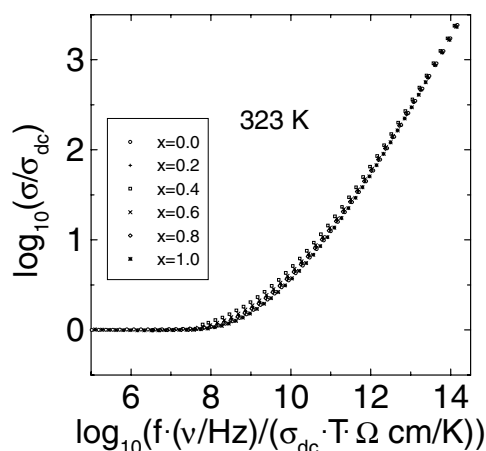
Figure 7. Scaled conductivity spectra of $0.3[x\mathrm{Li_2O}\cdot(1-x)\mathrm{Na_2O}]\cdot0.7\mathrm{B_2O_3}$ glasses at 323 K.

In figure 7 we present frequency-dependent conductivities of glassy $0.3[x\mathrm{Li_2O}\cdot(1-x)$ $\mathrm{Na_2O}]\cdot0.7\mathrm{B_2O_3}$ measured for different x *at a fixed temperature*, namely 323 K. In order to compare the shapes of the spectra, all data are presented in a normalized fashion. To make the spectra coincide at high frequencies we have, besides the Summerfield scaling, also used a scaling factor f, ranging between 0.5 and 1. The spectra of figure 7 corroborate the trend already reported in [37]. Starting with the binary sodium borate glass where $x = 0$, the transition into the dispersive regime becomes more and more gradual with increasing x until the composition $x = 0.4$ is reached. With further increase of x, the transition becomes less gradual again. Finally, the shape of the conductivity spectrum of the binary lithium borate glass coincides with the binary sodium borate glass.

Figures 8(a) and (b) are scaled representations of several conductivity isotherms of the binary glass $0.3\mathrm{Na_2O}\cdot0.7\mathrm{B_2O_3}$ and of the ternary glass $0.18\mathrm{Li_2O}\cdot0.12\mathrm{Na_2O}\cdot0.7\mathrm{B_2O_3}$, respectively. In both cases, the Summerfield scaling has been applied. Comparing figures 8(a) and (b), we encounter both similarities and differences. The two glasses agree in displaying a first derivative, $\partial\log(\sigma(\nu))/\partial\log(\nu)$, that increases with frequency, tending towards unity. This is also well in line with the shapes of conductivity spectra of many other solid electrolytes such as $\mathrm{B_2O_3}\cdot0.56\mathrm{Li_2O}\cdot0.45\mathrm{LiBr}$; cf figure 1. On the other hand, the two glasses differ regarding the preservation of the shape of their conductivity spectra when the temperature is changed. For the single-cation glass, the shape turns out to be temperature invariant, resulting in a single master curve in the scaled representation; see figure 8(a). As for $\mathrm{B_2O_3}\cdot0.56\mathrm{Li_2O}\cdot0.45\mathrm{LiBr}$—see figure 1—the time–temperature superposition principle and the Summerfield scaling are again found to be valid.

In contrast to the case for figure 8(a), we see in figure 8(b) that different isotherms of the mixed-alkali glass *do not* collapse onto a single master curve. Obviously, the shape of the conductivity spectra is temperature dependent. In the following section, this effect will be discussed in more detail.

5. Mixed-cation glasses: discussion

We have reported on *two* mixed-alkali effects, concerning changes in the shapes of frequency-dependent conductivities that occur along with variations of *composition* and *temperature*.
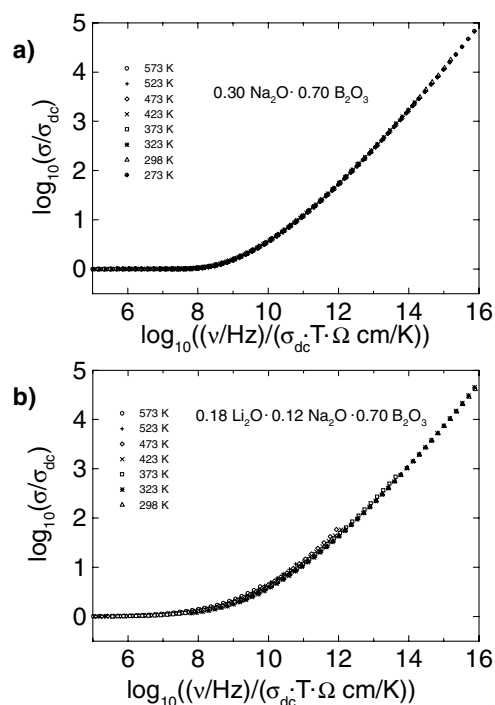
Figure 8. Scaled conductivity spectra of glassy (a) $0.3Na_2O \cdot 0.7B_2O_3$ and (b) $0.18Li_2O \cdot 0.12Na_2O \cdot 0.7B_2O_3$.

In the following, these effects will be quantified by application of a one-parameter procedure that has been established recently, within the framework of the CMR.

As shown in figure 7, the shapes of the mixed-alkali conductivity spectra strongly vary with composition. In order to quantify this effect, we have determined the values of the parameter K needed to obtain excellent fits to the experimental spectra. The results are displayed in figure 9. Evidently, the parameter K shows a pronounced mixed-alkali effect with a maximum at $x = 0.4$. The maximum of K occurs at the same composition where the dc conductivity passes through a minimum.

In the CMR model the parameter K appears to be linked to the effective number density of mobile ions. The smaller the number density, the higher the value of K. Accordingly, spectra of glasses and crystals with small concentrations of mobile cations are reproduced by model spectra with larger K-values than glasses and crystals with high cation contents. In a mixed-alkali glass system such as $0.3[xLi_2O \cdot (1 - x)Na_2O] \cdot 0.7B_2O_3$, however, the total number of cations remains constant for all glass compositions. Nevertheless, figure 9 suggests that the effective number of mobile ions should be strongly reduced in a mixed-alkali glass as compared to the binary glasses. This can be understood in the framework of the dynamic structure model (DSM) developed by Bunde *et al* [38]. In the DSM, each cation species creates its own chemical environment when a solid glass is formed from a melt. Therefore, a Li site in a glass differs from a Na site. As each cation species prefers to migrate via pathways of sites adjusted to its own requirements, the ionic mobility is drastically reduced if the pathways of the respective species interfere with each other. This picture readily explains the strong reduction of the effective number of mobile ions in mixed-alkali glasses.
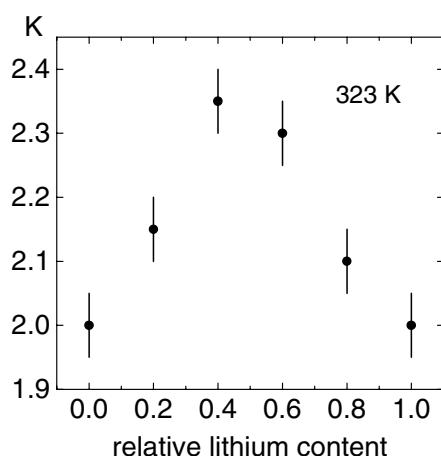
Figure 9. *K*-parameter values resulting from fits of the CMR model to conductivity spectra of $0.3[x\text{Li}_2\text{O}\cdot(1-x)\text{Na}_2\text{O}]\cdot 0.7\text{B}_2\text{O}_3$ glasses at 323 K.

In the following, we consider the *temperature dependence* of the conductivity spectra. As discussed in the previous section, the shape of the conductivity spectra of the single-cation glasses does not change with temperature—see figures 2(b) and 8(a)—which implies that temperature variations affect the ion dynamics only by changing the rates of the hopping processes, while the mechanism and the number of ions involved remain unchanged.

The conductivity spectra of the mixed-alkali glasses which do not collapse onto a master curve—see figure 8(b)—can also be described by the CMR, at least formally. The experimental spectra of glassy $0.18\text{Li}_2\text{O}\cdot 0.12\text{Na}_2\text{O}\cdot 0.7\text{B}_2\text{O}_3$ are presented in figure 10 along with curves obtained using the CMR. In contrast to the case for the single-cation glasses, where a constant *K*-value of about 2 has been used to describe *all* conductivity isotherms, the value of *K* is found to *increase with temperature* in the mixed-alkali glasses. The higher the temperature, the more gradual the transition from the dc plateau to the dispersive regime. This breakdown of the time–temperature superposition principle is a new kind of mixed-alkali effect. Figure 11 shows the CMR parameter *K* as a function of composition at different temperatures. It is obvious that the strongest changes of the spectral shape with temperature occur for compositions $x = 0.4$ and 0.6. The reason that the effect was not detected in a previous study on the same glass system [37] lies in the more limited ranges in frequency and temperature.

An explanation of the temperature-dependent shape of the mixed-alkali conductivity spectra may be provided by the assumption of differently activated mobilities of the two different ionic species. As mentioned earlier, ionic transport is dominated by the more mobile ionic species. This applies on either side of the diffusion crossover point [39]. However, there is a lack of radio-tracer experiments concerning the temperature dependences of the respective mobilities in mixed-alkali glasses. *A priori*, of course, there is no reason that the different cation species should have identical activation energies of their mobilities.

Let us, therefore, assume that, in a given mixed-alkali glass, the mobilities of the two species are slightly differently activated. In a simplified approach we also assume that each of the two species contributes separately to the overall conductivity. The total conductivity spectrum is then easily constructed at each temperature by adding the individual spectra of the two species. It turns out that even if the individual spectra follow the time–temperature superposition principle, the shape of the total spectra will be temperature dependent. This is in agreement with the actual experimental findings.
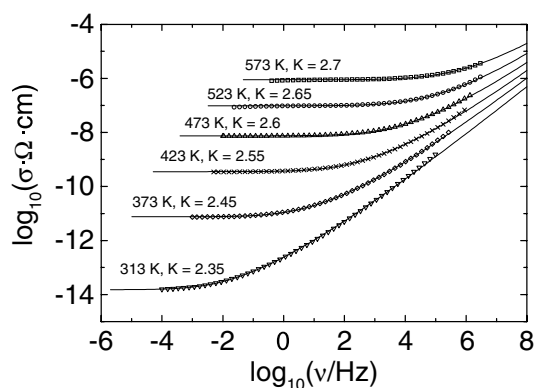
Figure 10. Experimental conductivity spectra of glassy $0.18Li_2O \cdot 0.12Na_2O \cdot 0.7B_2O_3$ at various temperatures and fits based on the CMR model. The value of the parameter K increases with temperature.

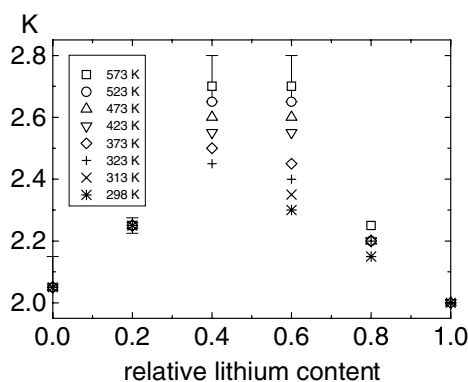**Figure 11.** K-parameter values resulting from fits of the CMR model to conductivity spectra of $0.3[xLi_2O \cdot (1-x)Na_2O] \cdot 0.7B_2O_3$ glasses at different temperatures.

If the mobilities of the two cation species were Arrhenius activated, but with different activation energies, the sum of these two contributions should deviate from the Arrhenius law which is usually used to describe the temperature dependence of $\sigma_{dc}T$. Instead of a straight line, one would expect a slightly concave curve. We have, therefore, carefully checked the validity of the Arrhenius law for the experimental dc conductivities of our mixed-alkali glasses. We find the experimental data basically well described by an Arrhenius law. However, very small deviations from a straight line are detectable at our lowest and highest temperatures. Similar deviations have been reported by Mehrer [39], Namikawa [40] and Jain *et al* [41]. Nevertheless, dc conductivity measurements over an even larger temperature range are desirable before drawing any further conclusions.

An alternative interpretation for the concentration- and temperature-dependent shapes of the mixed-alkali conductivity spectra may be given in terms of the concept of matrix-mediated coupling developed by Ingram and co-workers [42]. Within this model, hops of dissimilar cations (in this case Li⁺ and Na⁺) can become coupled through the mediation of matrix relaxations. As such coupling intensifies as the temperature is raised towards the glass transition temperature T_G, the changes in the shape of the conductivity spectra could be

attributed to such a mechanistic change. Temperature-dependent tracer measurements would surely shed light on the temperature dependence of ionic mobilities in mixed-alkali glasses.

6. Summary and outlook

In this paper, we have analysed complete conductivity spectra of three single-cation-conducting glasses, extending over many decades on the frequency scale. We have shown that in all cases the conductivity spectra are consistently described by a superposition of only two contributions. One of them determines the conductivity spectra at frequencies below some gigahertz and reflects the hopping dynamics of the mobile ions. It is well reproduced within the framework of the CMR. The other contribution is caused by vibration-like movements of charged particles. It is only slightly temperature dependent and its shape strongly depends on the respective glass. Here, marked differences between the three glasses have been highlighted and discussed. However, more theoretical work is needed to fully understand the dynamics occurring on a picosecond timescale.

In contrast to the conductivity spectra of single-cation glasses which follow the time–temperature superposition principle, featuring a temperature-invariant shape, the conductivity spectra of the mixed-alkali glasses studied here have shapes that are found to change with temperature. To explain the effect, we suggest differently activated mobilities of the two different ionic species. All spectra of glassy $0.3[x\mathrm{Li_2O}\cdot(1-x)\mathrm{Na_2O}]\cdot 0.7\mathrm{B_2O_3}$ presented are well described within the framework of the concept of mismatch and relaxation. The variation of the model parameter K with composition suggests that the effective number of mobile ions is strongly reduced in a mixed-alkali glass as compared to the binary glasses. This can be understood in the framework of the dynamic structure model [38] in which each cation species prefers to migrate via pathways of sites adjusted to its own requirements.

Acknowledgments

References

[1] Cramer C, Grimsditch M and Saboungi M-L 1999 *J. Phys. Chem.* B **103** 4018
[2] Ingram M D, Chryssikos G D and Kamitsos E I 1991 *J. Non-Cryst. Solids* **1089** 131
[3] Kamitsos E I, Kapoutsis J A, Chryssikos G D, Hutchinson J M, Pappin A J, Ingram M D and Duffy J A 1995
     Phys. Chem. Glasses **36** 141
[4] Rau C, Armand P, Pradel A, Varsamis C P E, Kamitsos E I, Granier D, Ibanez A and Philippot E 2001
     Phys. Rev. B **63** 184204
[5] Janssen M and Eckert H 2000 *Solid State Ion.* **136/137** 1007
[6] Ratai E, Janssen M and Eckert H 1998 *Solid State Ion.* **105** 25
[7] Funke K and Cramer C 1997 *Curr. Opin. Solid State Chem. Sci.* **2** 483
[8] Funke K and Cramer C 2001 *Encyclopedia of Materials, Science and Technology* vol 1, ed K H J Buschow,
     R W Cahn, M C Flemings, B Ilschner, E J Kramer and S Mahajan (Oxford: Elsevier) pp 189–94
[9] Jonscher A K 1977 *Nature* **267** 673
[10] Lee W-K, Liu J F and Nowick A S 1991 *Phys. Rev. Lett.* **67** 1559
[11] Nowick A S, Vaysleyb A V and Liu W 1997 *Solid State Ion.* **105** 121
[12] Funke K, Roling B and Lange M 1997 *Solid State Ion.* **105** 195
[13] Schrøder T B and Dyre J C 2000 *Phys. Rev. Lett.* **84** 310

[14] Sidebottom D L, Green P F and Brow R K 1997 *Phys. Rev.* B **56** 170
[15] Cramer C, Brückner S, Gao Y and Funke K 2002 *Phys. Chem. Chem. Phys.* **4** 3214
[16] Summerfield S and Butcher P N 1985 *J. Non-Cryst. Solids* **77/78** 135
[17] Summerfield S 1985 *Phil. Mag.* B **52** 9
[18] Roling B, Funke K, Happe A and Ingram M D 1997 *Phys. Rev. Lett.* **78** 2160
[19] Roling B and Martiny C 2000 *Phys. Rev. Lett.* **85** 1274
[20] Cramer C, Brückner S, Gao Y, Funke K, Belin R, Taillades G and Pradel A 2002 *J. Non-Cryst. Solids* **307–310** 905
[21] Strom U, Hendrickson J R, Wagner R J and Taylor P C 1974 *Solid State Commun.* **15** 1871
[22] Strom U and Taylor P C 1977 *Phys. Rev.* B **16** 5512
[23] Cramer C and Buscher M 1999 *Solid State Ion.* **105** 109
[24] Krishnaswami S, Jain H, Kamitsos E I and Kapoutsis J A 2000 *J. Non-Cryst. Solids* **274** 307
[25] Ngai K L, Cramer C, Saatkamp T and Funke K 1996 *Workshop on Non-Equilibrium Phenomena in Supercooled Fluids, Glasses and Amorphous Materials* vol 3, ed M Giordano, D Leporini and M P Tosi (Singapore: World Scientific) pp 3–21
[26] Brunklaus S and Cramer C 2002 unpublished results
[27] Ngai K L 1979 *Comment. Solid State Phys.* **9** 127
[28] Ngai K L 1980 *Comment. Solid State Phys.* **9** 141
[29] Funke K 1987 *Z. Phys. Chem.* **154** 251
[30] Funke K 1993 *Prog. Solid State Chem.* **22** 111
[31] Funke K and Wilmer D 1999 *Mater. Res. Soc. Symp. Proc.* **548** 403
[32] Funke K and Wilmer D 2000 *Solid State Ion.* **136/137** 1329
[33] Funke K and Wilmer D 2001 *Radiat. Eff. Defects Solids* **155** 387
[34] Funke K, Brückner S, Cramer C and Wilmer D 2002 *J. Non-Cryst Solids* **307–310** 921
[35] Funke K, Banhatti R D, Brückner S, Cramer C, Krieger C, Mandanici A, Martiny C and Ross I 2002 *Phys. Chem. Chem. Phys.* **4** 3155
[36] Murugavel S and Roling B 2002 *Phys. Rev. Lett.* **89** 195902
[37] Roling B, Happe A, Ingram M D and Lange M 1999 *J. Phys. Chem* B **103** 4122
[38] Bunde A, Ingram M D and Maass P 1994 *J. Non-Cryst. Solids* **172–174** 1222
[39] Imre A, Voss S and Mehrer H 2002 *Phys. Chem. Chem. Phys.* **4** 3219
[40] Namikawa H 1975 *J. Non-Cryst. Solids* **18** 173
[41] Jain H, Downing H L and Petersen N L 1984 *J. Non-Cryst. Solids* **64** 335
[42] Bandaranayake P W S K, Imrie C T and Ingram M D 2002 *Phys. Chem. Chem. Phys.* **4** 3209